Real-in time CT test of the rock meso-damage propagation law

GE Xiurun (葛修润)[1,2,4], REN Jianxi (任建喜)[1,2,3], PU Yibin (蒲毅彬)[1], MA Wei (马 巍)[1] & ZHU Yuanlin (朱元林)[1]

1. State Key Laboratory of Frozen Soil Engineering, LIGG, Chinese Academy of Sciences, Lanzhou 730000, China;
2. Institute of Rock and Soil Mechanics, Chinese Academy of Sciences, Wuhan 430071, China;
3. Xi'an University of Science & Technology, Xi'an 710054, China;
4. Institute of Rock & Soil Mechanics & Engineering, Shanghai Jiaotong University, Shanghai 200030, China
Correspondence should be addressed to Ge Xiurun

Received October 21, 2000

Abstract The real-in time computerized tomography (CT) test of the meso-damage propagation law of the whole rock failure process has been completed using the newest specified triaxial loading equipment corresponding to the CT machine. Through the CT scanning, the clear CT images which include the microholes (microcracks) compressed→growth→bifurcation→development→crack fracture →the rock sample failure→unloading in the different stress states were obtained. The CT values, CT images and other data have been analysed. The initial damage effect coefficient has been loaded, and a new damage variable based on CT value defined. The initial rock damage propagation law is given here.

Keywords: **rock, CT test, damage propagation, meso-scale, damage variable.**

At present, the rock damage mechanic characteristics are extensively concerned as one of the important problems in rock mechanics. Meso-damage mechanics deals with the different damage shapes, distributions and damage evolution characteristics of the particle, crystal grain, micro-crack and void in materials. A study on the meso-damage propagation law not only can provide important experimental information on macro-damage theory, but also is helpful for understanding the rock failure mechanism. Dougill first applied the damage mechanics to rock materials. Krajcionvie et al. revealed characteristics of the rock damage and established several corresponding damage models and damage theories. Xie studied the rock and concrete damage mechanics[1]. Using a micro-loading equipment, Ling completed the dynamic test research of the rock damage propagation law with a scanning electron microscope, and advanced a brittle rock mesco-damage model[2]. Wu et al. and Ma et al. studied the creep characteristics of frozen soil using CT test technology[3,4]. Kawakata et al. and Yang studied the rock initial meso-damage characteristics with the CT scanning test, and initially studied the rock damage propagation law[5,6]. It should be pointed out that in their CT test, the rock sample was predamaged on an MTS machine, then unloaded and finally scanned using the CT machine. In this work, using the newest CT loading equipment, the CT real-in time scanning tests of rock meso-damage propagation law in the complete process under the triaxial (uniaxial) compression have been performed. This paper aims to investigate the rock failure law, establish the rational rock damage evolution equation and explore rock damage constitutive relation based on statistics so as to provide some data for rock masses strength analysis and deformation control.

1 CT real-in time test of the rock damage propagation law

1.1 Testing equipment

The configuration of the specially developed triaxial loading equipment for the CT machine is: Ø240 × 1000 mm, the interior diameter of axial pressure chamber Ø142 mm, and the maximum axial load 400 KN, with the largest confining pressure 20 MPa, axial run distance 400 mm measuring range of deformation sensor 0—50 mm, and accuracy degree 0.31%. The equipment can also be used to complete the rock failure test under the triaxial (uniaxial) compression with the international standard cylinder rock sample (Ø50 × 100 mm) and to complete the failure test of the soil sample (Ø61.8 × 150 mm). And it can also be used to perform dynamic scan test to research the sample deformation law. The testing equipment is installed in the CT scan region during the process of the test. In order to reduce the influence on the test results, the triaxial loading chamber was made of premium light metal material LY12 instead of heavy metal materials. The specially designed triaxial (uniaxial) loading system is the necessary accessory for the CT machine at the State Key Laboratory of Frozen Soil Engineering of China. The first author of this paper headed the gerenal design work.

The type of the CT machine is a spiral scanning Siemens Somaton plus X-ray with a spatial resolution 0.35 mm × 0.35 mm, volume resolution 0.12 mm^3 (1 mm slice) and density contrast resolution 0.3% (3 Hu). The research scale of meso-mechanics ranged from angstrom unit to millimeter[6]. In the rock meso-damage progapation test Siemens Somation plus type CT machine satisfied the lower bound of the scale range of meso-mechanics.

1.2 Rock samples

The rock samples were sandstone (with average density 2.45 g/cm^3) and coal (with average density 1.47 g/cm^3), sampled from the Nanqiao of the Shannxi Pubai Mine from March 28 to April 4, 1999.

1.3 Testing process

The CT test was carried out in the State Key Laboratory of Frozen Soil Engineering from April 15 to April 27, 1999. The sandstone samples were used to study the rock meso-damage propagation law under triaxial (uniaxial) compression with CT real-in time scanning test. Using the coal samples the meso-damage propagation under triaxial compression was tested. For each sample there were three or four cross sections from top to bottom. Each of them was scanned by the CT machine to observe the graphic changes in the growth, bifurcation, development, fracture, unloading in the different stress states, and the rock failure phenomena in meso-scale.

2 Analysis of the test results

2.1 Analysis of the rock damage evolution

(1) The test results of No. 5 sandstone may be taken as an example (table 1). No. 5 sandstone had four cross sections, each section being scanned 8 times. Altogether 32 images were obtained. Fig. 1 is the image of the sample installed in the pressure chamble. Each section was 3 mm deep and the rate of strain was $2.75 \times 10^{-5}/s$. This is a case of quasistatic loading test. The test lasted 55 min. Figs. 3((a)—(d))—10((a)—(d)) are corresponding to the sample CT images of the four scan sections from top to bottom under different stress conditions. In table 2 are given the corresponding stress states of 8 times scanning test. The relationship between

$(\sigma_1 - \sigma_2)$ and ε_1 and the plots of scan test are shown in fig. 2. Table 3 gives the test results of each scan section of No. 5 sandstone.

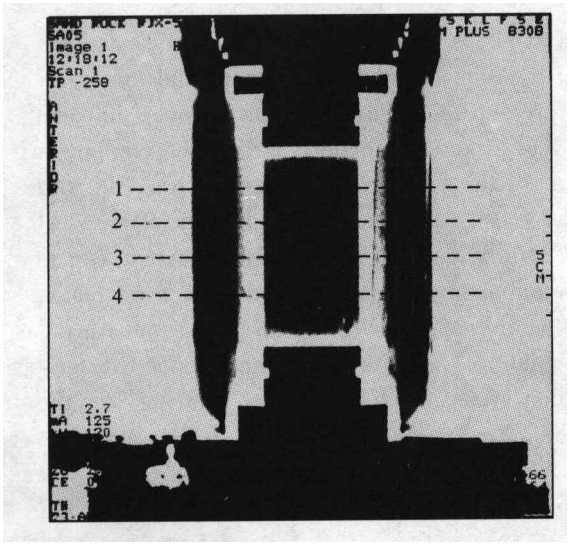

Fig. 1. CT image of No. 5 sandstone sample installed in the triaxial testing cell.

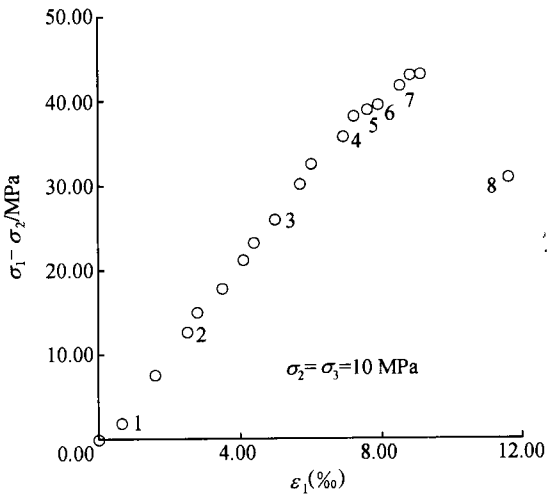

Fig. 2. Relationship curve of $(\sigma_1 - \sigma_2) \sim \varepsilon_1$ (the number on curve corresponding to scan order in table 2).

Table 1 Scan test conditions

Voltage/kV	Current/mA	Time/s	Label	Depth/mm	Amplifying factor	*X*/*Y*
137	440	2	OM	3	6.5	10/4

Table 2 Stress state of each scan test ($\sigma_2 = \sigma_3 = 10$ MPa)

Scan order	σ_1/MPa	$(\sigma_1 - \sigma_2)$/MPa	ε_1(‰)
1	11.88	1.88	0.63
2	22.63	12.63	2.5
3	35.92	25.92	5.0
4	45.66	35.66	6.9
5	48.85	38.85	7.6
6	49.47	39.47	7.9
7	51.71	41.71	8.5
8	40.79	30.79	11.6

Table 3 Test results of each scan section of No. 5 sandstone

Scan order	1st scan section		2nd scan section		3rd scan section		4th scan section		Rock sample	
	ME	*SD*	*ME*	*SD*	*ME*	*SD*	*ME*	*SD*	$\frac{1}{4}\sum_{i=1}^{4} ME/\Delta ME$	$\frac{1}{4}\sum_{i=1}^{4} SD/\Delta SD$
1	1 625.6	98.95	1 630.0	102.07	1 592.6	105.01	1 582.3	172.03	1607.63	119.52
2	1 626.6	104.52	1 633.6	104.51	1 598.2	105.10	1 583.5	172.86	1610.48/2.85	121.75/2.23
3	1 627.6	105.50	1 634.3	104.74	1 601.1	104.94	1 584.5	166.57	1612.05/4.42	120.44/10.92
4	1 626.6	105.63	1 634.2	102.19	1 602.3	104.07	1 585.2	166.76	1612.08/4.45	119.81/0.29
5	1 625.9	104.35	1 632.0	101.07	1 601.9	101.05	1 584.8	166.67	1611.15/3.52	118.27/ - 1.25
6	1 624.5	101.54	1 627.4	100.71	1 596.7	97.11	1 581.5	165.44	1607.53/ - 0.1	116.20/ - 3.32
7	1 622.9	97.53	1 621.5	99.87	1 591.0	98.84	1 578.7	165.74	1603.45/ - 4.18	115.50/ - 4.027
8	1 609.9	91.56	1 604.3	113.37	1 576.9	115.51	1 565.4	183.29	1589.13/ - 18.5	129.93/10.41

ME, the CT number; $\frac{1}{4}\sum_{i=1}^{4} ME$, the CT number of rock sample; ΔME, the variance in rock sample CT number between different stress states and the first scan; *SD*, the variance in the CT number; $\frac{1}{4}\sum_{i=1}^{4} SD$, the variance of rock sample CT number; ΔSD, the variance in rock sample CT number between different stress states and the first scan.

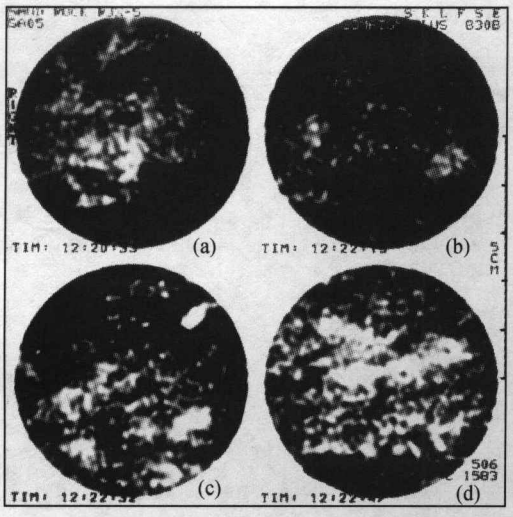

Fig. 3. CT image of each scan section ($\sigma_1 = 11.88$ MPa).

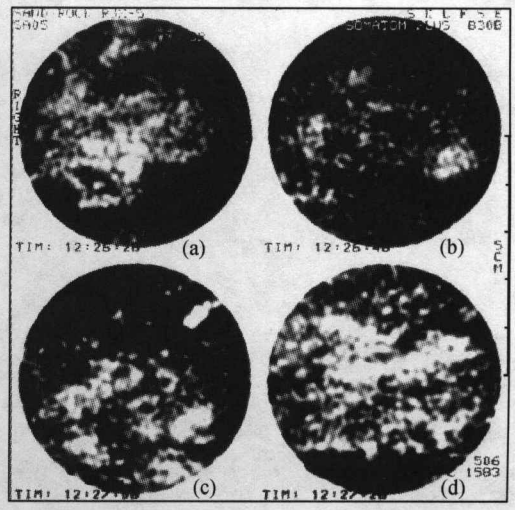

Fig. 4. CT image of each scan section ($\sigma_1 = 22.63$ MPa).

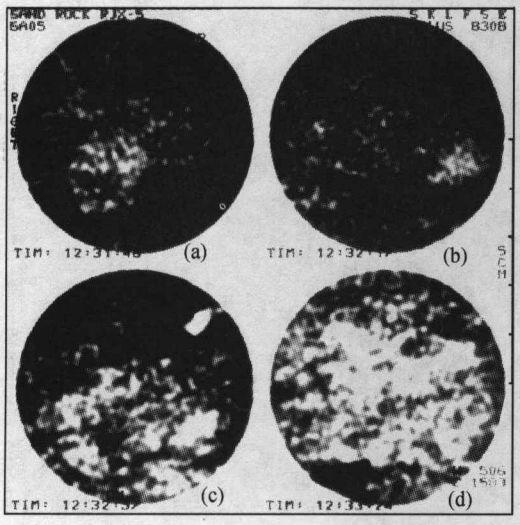

Fig. 5. CT image of each scan section ($\sigma_1 = 35.92$ MPa).

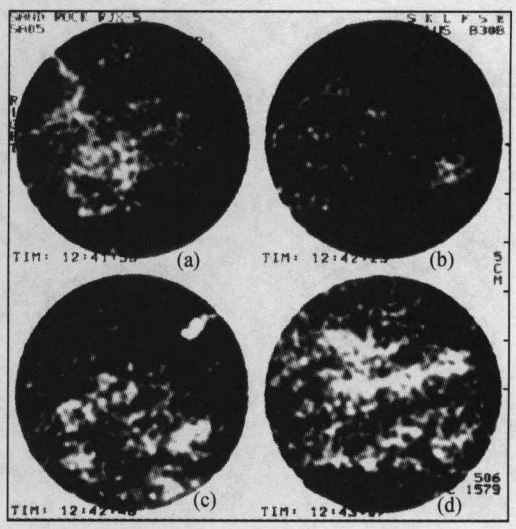

Fig. 6. CT image of each scan section ($\sigma_1 = 45.66$ MPa).

Table 3 shows that when σ_1 ranges from 11.88 to 35.92 MPa, both the CT values of four scan sections and the CT value of the rock sample increase. In fact, the rock microcracks and holes (the initial damage) begin to be closed, the rock sample is compressed, and the rock comes denser. On the other hand, as shown in figs. 3 and 4, some white regions (low density regions) are converted to black ones in these CT images (high density regions). Note that the CT images obtained with the CT machine are very clear because of the large gray scale. But as the CT images in this paper (figs. 3—10) are copies of the CT photographs, the gray scale is not so distinct. This affects the quality of CT images. When $\sigma_1 = 35.92$ MPa, CT images in fig. 5(a), (b) show that a few cracks begin to grow and bifurcate. And when σ_1 reaches 45.66 MPa, the CT value of the first and second scan sections begin to decrease and the microcracks begin to lengthen and bifurcate, and there are lots of microcracks growing (fig. 6(a), (b)). At the same

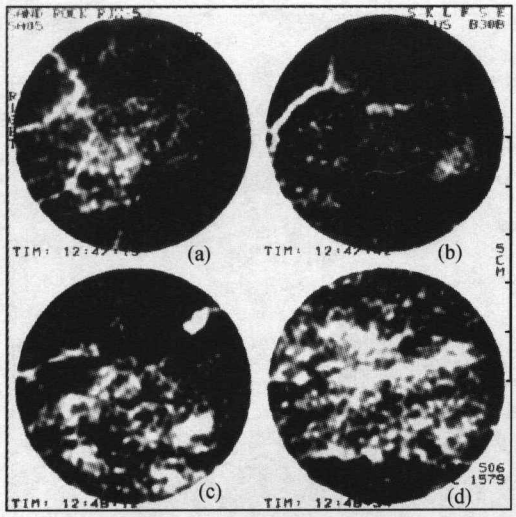

Fig. 7. CT image of each scan section ($\sigma_1 = 48.85$ MPa).

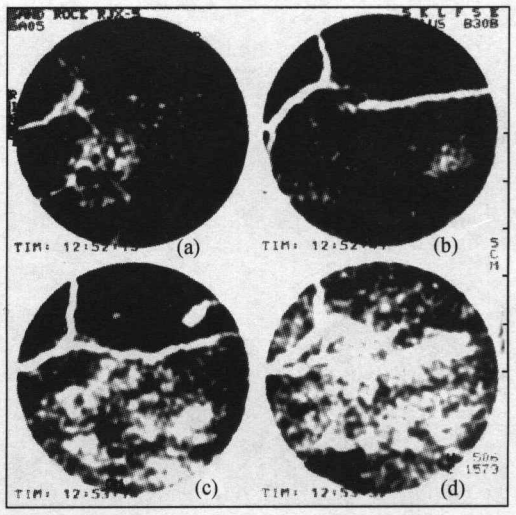

Fig. 8. CT image of each scan section ($\sigma_1 = 49.47$ MPa).

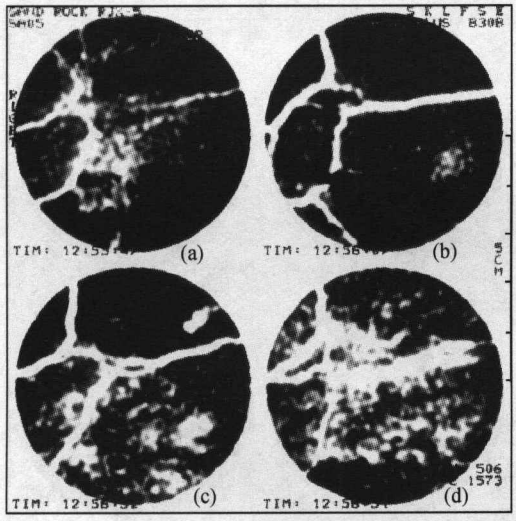

Fig. 9. CT image of each scan section ($\sigma_1 = 51.71$ MPa).

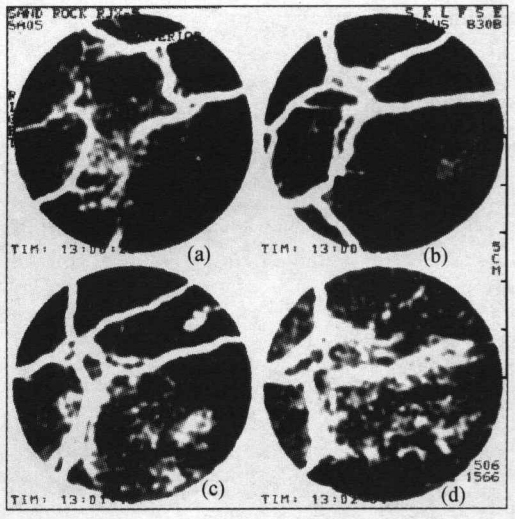

Fig. 10. CT image of each scan section ($\sigma_1 = 40.79$ MPa).

time, images in fig. 6(a,b) show that there is an omen of the new microcracks beginning to grow in the last scanning. Light plots occur in some regions of scanning sections (low density regions). On the other hand, the CT values of the third and fourth scan sections have increased a bit and there are a few microcracks growing, suggesting that there are different damage phenomena in different sections of the same sample compressed by the same loading. This is heterogeneity of the rock damage evolution.

When σ_1 reaches 48.85 MPa, the microcracks grown in the last stage begin to lengthen, and more new microcracks begin to grow. Both of the CT value of each scan section and the CT value of rock sample (the CT value of rock sample is defined by the average value of each scan section in a stress state) begin to decrease. When σ_1 rises from 48.85 to 49.47 MPa, in this stage, the CT values of each section and rock samples obviously decrease, the microcracks of the first scan section continue lengthening (fig. 8(a)), and the microcracks of the second and third

scan sections begin to bifurcate, lengthen and nearly penetrate (fig. 8(b, c)). Many microcracks of the fourth scan section begin to bifurcate, and there occurs a "Z" type crack penetrating the left upper part of CT image in fig. 8(d). When σ_1 rises to 51.71 MPa, every section has many penetrating microcracks. This stage is the failure omen stage, and it is the stage of fastest evolution. When σ_1 approaches to the peak strength near 53.12 MPa, cracks completely penetrate, and in each section 2 or 3 maincracks occur which cause rock sample to fail . When σ_1 is unloaded from peak value to 40.79 MPa, several penetrating maincracks begin to broaden (fig. 10).

(2) Figs. 5—10 show that the initial extending direction of cracks parallels the direction of the maximum main-stress or forms a mini-angle, but the further extending directions are different. The darkest points in the high density regions have special meanings for the damage evolution. The bifurcation of cracks will form around the high density particles. Figs. 9 and 10 show that the main fracture surface is not a plane in the triaxial compression test, but is a bent surface. The phenomenon of shear-expansion happens because of the sliding motion of the material on the two sides of the maincracks in the bent surface.

(3) In order to study the law of the cracks growth, bifurcation and extension in the maincrack regions, the region containing maincracks of the second scan section in the left upper part is taken for detailed analyses (fig. 10(b)).

Through analysing the test results of the "dangerous area" of the second section (3.47 cm^2), the following laws can be found. In the stage of σ_1 from 11.88 to 35.92 MPa, the CT value is increased up to 2.47‰ in the region where the microcracks are grown and developed. But, in the meantime, the CT value of the whole rock sample in the same stage is nearly the same. When σ_1 ranges from 35.92 to 45.66 MPa, the CT value of rock sample is decreased about 2.55‰. When σ_1 ranges from 45.66 to 48.85 MPa, the CT value of the area decreases 5.66‰, but the variance begins to increase. When σ_1 ranges from 48.85 to 51.71 MPa, microcracks penetrate ecah other, the damage evolution speed is the fastest, the CT value of this area decreases nearly 20.76‰, the variance increases 122% , but the CT value of No. 5 rock sample in the same stage only decreases 4.87‰. When σ_1 nearly approaches to the peak value, most cracks are penetrated and fractured, showing that the final failure of rock material is determined by one or more maincracks. The area with more rock initial damages in the second scan section of No. 5 sample is apt to become an area where the phenomena of the microcracks growth, development, fracture and failure appear more easily. It is the very rock damage propagation localization phenomenon in the CT images.

(4) The failure type of the No. 5 sandstone sample is damage fracture under the triaxial compression. Analysis of the relation between CT images (fig. 5) and the stress state (fig. 2), shows that the stress level of $\sigma_1 = 35.92$ MPa for No. 5 sandstone sample seems to be the barrier, beyond which the damage will occur, because there were few microcracks grown in the first scan section (fig. 5) when $\sigma_1 = 35.92$ MPa, and the CT value of the first scan section began to decrease.

(5) Comparisons of the CT scan results of the uniaxial test and the triaxial test show that the peak value of σ_1 of the uniaxial test is less than that of the triaxial test with the same type rock samples, and the peak value of ε_1 of the triaxial test is also obviously less than that of the uniaxial test. CT images show that the microcracks growth stages in the triaxial test and the uniaxial test are different. Because of the effect of the confining pressure, microcracks of the triaxial test are

larger than that of the uniaxial test in number. In the uniaxial compression, most rock samples failures are brittle failures. But in the triaxial compression test, the higher the confining pressure, the more obvious the plastic failure characteristics (table 4).

Table 4 CT value analysis of "dangerous area" of second scan section

Scan order	*ME*	*ΔME*	*SD*	*ΔSD*
1	1641.3		41.57	
2	1643.7	2.4	40.67	-0.9
3	1645.8	4.5	38.74	-2.83
4	1641.6	0.3	40.80	-0.77
5	1632.3	-9.0	48.84	7.27
6	1613.2	-28.1	79.6	38.03
7	1598.4	-42.9	92.30	50.73
8	1575.8	-65.5	106.35	64.78

ME, the CT number; ΔME, variance in the rock sample CT number between different stress state and the first scan; *SD*, the variance in the CT number; ΔSD, variance in the rock sample CT number between different stress state and the first scan.

(6) As described in the preceding paragraph, when $\sigma_1 = 35.92$ MPa, namely $(\sigma_1 - \sigma_2) = 25.92$ MPa, the sign of growth and bifurcation of a few microcracks begins to emerge. If the $(\sigma_1 - \sigma_2) = 41.71$ MPa of peak strength is regarded as the cardinal number, then this stress value is 62.1% of the peak strength. In ref. [8], according to the testing results of marco-mechanics, 65%—70% of the peak strength value can be regarded as the threshold value of fatigue failure of rock under cyclic load. Below this threshold value, the fatigue failure would not happen. It is reported that the threshold value of rheology failure of rock was about the 65% of peak strength. It is worth noting that the conclusions are based on marco test of mechanics characteristics. The meso-mechanics testing results of this work show that when the stress value of the sandstone of the coal mine in Nanqiao is below 62% of peak strength value, the rock material is compressed, then the value of the rock density is raised, but when the stress exceeds this value, an essential change takes place. Obviously, a few microcracks begin to lengthen, bifurcate and there are a lot of microcracks beginning to grow. It can be inferred that there is an internal relation between the turning point of the microcracks propagation, bifurcation and growth based on the meso-mechanics and the mechanism of the fatigue failure and the rheology failure of rock. In this test, as only a few rock samples were used, and the scan sections and the scan times were limited in number, much is left to be done. However, we think a thorough study of this problem will make it possible to establish the internal realtions between the rock meso-mechanics and the marco-mechanics characteristics, thus providing something new for the marco-mechanics.

2.2 Definition of the damage variable

By virtue of a mathematics model, ref. [6] gave the following damage variable:

$$D = -\frac{1}{m_0^2}\frac{\Delta\rho}{\rho_0}, \tag{1}$$

where m_0 is the spatial resolution of the CT machine, $\Delta\rho$, the rock density change in the process of the rock damage evolution, and ρ_0 the initial rock density.

Obviously, the key problem of defining damage variable D is determination of $\Delta\rho$. According to the CT theory, the number of H_{rm} (H_{rm} is the rock CT number) is in direct proportion to the rock density, the distribution of H_{rm} essentially reflects the distribution of rock density, and the value of H_{rm} is in direct proportion to the absorbed factor μ of rock to X-ray, so

$$H_{rm} = k \cdot \mu, \tag{2}$$

where k is a constant.

Assume that each type damage (void and microcrack) is filled up only with air and ignore the effect of water. Then

$$\mu = \mu^m \rho = (1 - \alpha)\rho_b \mu_b^m + \alpha \rho_a \mu_a^m, \tag{3}$$

where ρ is the rock density of some stress state, ρ_b, ρ_a are the densities of non-damaged rock material and air, α is the pore density, and μ_b^m, μ_a^m are the absorbed factor of rock to X-ray and air to X-ray.

The material density in a space resolving unit reads

$$\rho = (1 - \alpha)\rho_b + \alpha \rho_a. \tag{4}$$

With formulae (2) and (3), the parameters μ, α can be calculated out. Assuming that the density of air $\rho_a = 0$, and the CT number of air $H_a = -1000$, and substituing it into formula (4), through calculation we have

$$\Delta\rho = \rho - \rho_0 = \frac{1\,000 + H_{rm}}{1\,000 + H_{rmb}}\rho_b - \rho_0, \tag{5}$$

where H_{rmb} is the CT value of non-damaged rock.

Rocks are a kind of natural materials. Generally speaking, there is no undamaged rock in the world. So, it is difficult to define the ρ_b and H_{rmb} in formula (5). The purpose of this research is to investigate the rock damage evolution law, and the rock density change in the process of the rock damage propagation, so the density of the initial damage rock material ρ_0, the CT value H_{rm0} can be used to substitute ρ_b, H_{rmb}, and H_{rm0} can be defined as the rock initial damage characteristics CT test.

Here $\rho_0 = \rho_b$, $H_{rm0} = H_{rmb}$. Substituting them into formula (5), calculating out $\Delta\rho$, and then substituting $\Delta\rho$ into formula (1), we have

$$D = \frac{1}{m_0^2}\left(1 - \frac{1000 + H_{rm}}{1000 + H_{rm0}}\right). \tag{6}$$

Note that the effect of the initial damage cannot be accounted for in formula (6). This is not very rational. In order to account for the effect of the rock initial damage, the right side of formula (6) is multiplied by an initial damage effect factor e.

$$D = \frac{e}{m_0^2}\left(1 - \frac{1000 + H_{rm}}{1000 + H_{rm0}}\right). \tag{7}$$

Formula (7) gives a new damage variable based on the rock CT number, where $e > 1$. The value of e can be defined by fit test between the constitutive equation and the stress-strain curve obtained from the CT scan test. So D is easily calculated out from the rock CT value and e, and it is easy to obtain the rock damage evolution law. When calculating the damage variable D by CT value, in order to cancel out the effect of the hydraulic power oil and the sample scale, etc., the CT value must be modified through more rock failure CT scan tests.

Let it be noted that the meaning of formula (7) is very important. Bellomi (1978), Davis (1966) and Levaillant (1979) et al. defined the damage variable with the change value of the material density, but the $\Delta\rho$ was difficult to measure. This difficulty is solved in this paper. On the other hand, the effect of the rock meso-damage identification scale is corrected with the spatial resolution of the CT machine in formula (7).

4 Conclusions

(1) Using the newest triaxial loading test system developed by the authors, the real-in time CT scanning test of the rock meso-damage propagation law of the whole rock failure process under the triaxial (uniaxial) compression has been completed for the first time.

(2) Clear CT images are obtained which include the microholes (microcracks) compressed →growth→bifurcation→development→fracture→rock failure→unloading in the different stress states. The test results are satisfactory, showing that this equipment is successful.

(3) The newest triaxial loading CT test system provides an innovative testing method for studying the rock failure theory on meso-scale. The initial test results demonstrate that this method is practicable. It would actively motivate rock damage test technology. On the other hand, the development of the advanced meso-damage propagation law test technology would provide important test results for the macro-damage theory, and it can provide data for establishing the damage evolution equation and constitutive model to the research of rock failure law.

(4) In this paper, an initial damage effect factor is suggested, and a new damage variable based on the CT value is defined, thus making the analytic CT test quantitative and laying a basis for the establishment of the rock damage evolution equation and the constitutive model.

(5) A systimatical investigation of the rock damage evolution by the real-in time CT test and the further quantitative analysis of CT test results are in progress.

Acknowledgements This work was supported by State Key Laboratory of Frozen Soil Engineering, LIGG CAS (No. 9802).

References

1. Xie Heping, Rock and Concrete Damage Mechanics (in Chinese), Xuzhou: China University of Mining & Technology Press, 1990, 152—166.
2. Ling Jianming, Research on damage mechanics and time-dependent damage characteristics for jointed rock masses, Ph. D. Dissertation (in Chinese), Tongji University, 1992, 55—59.
3. Wu Ziwang, Ma Wei, Pu Yibin, Chang Xiaoxiao, Submicroscopic analysis on deformation characteristics in creep process of frozen soil, Chinese Journal of Geotechnical Engineering (in Chinese), 1997, 19(3): 1.
4. Ma Wei, Wu Ziwang, Pu Yibin et al., Monitoring the change of structures in frozen soil in triaxial creep process by CT, J. of Glaciology and Geocryology (in Chinese), 1997, 19(1): 52.
5. Kawakata, H., Cho, A. T., Yanagidani, M. S., The observation of faulting in westerly granite under triaxial compression by X-ray CT scan, Int. J. Rock Mech & Min. Sci., 1997, 34(3-4): 151.
6. Yang Gengshe, Zhang Changqing, Rock masses damage and identification (in Chinese), Xi'an: Shaanxi Science and Technology Press, 1998, 79—90.
7. Yang Wei, Meso-mechanics and meso-damage mechanics, Advances in Mechanics (in Chinese), 1992, 22(1): 1.
8. Ge Xiurun, Lu Yingfa, Fatigue failure and irreversible deformation of rock under cyclic load, Chinese Journal of Geotechnical Engineering (in Chinese), 1992, 14(3): 56.